



Ninjurin 1 has two opposing functions in tumorigenesis in a p53-dependent manner

Hee Jung Yang^a, Jin Zhang^{a,1}, Wensheng Yan^a, Seong-Jun Cho^b, Christopher Lucchesi^a, Mingyi Chen^c, Eric C. Huang^d, Ariane Scoumanne^a, Weici Zhang^e, and Xinbin Chen^{a,1}

^aDepartment of Surgical and Radiological Sciences, Schools of Veterinary Medicine and Medicine, University of California, Davis, CA 95616; ^bLow-Dose Radiation Research Team, KHNP Radiation Health Institute, Korea Hydro & Nuclear Power Co., LTD, Seoul 01450, South Korea; ^cDepartment of Pathology, University of Texas Southwestern Medical Center, Dallas, TX 75390; ^dDepartment of Pathology and Laboratory Medicine, School of Medicine, University of California, Davis, Sacramento, CA 95817; and ^eDivision of Rheumatology/Allergy and Clinical Immunology, School of Medicine, University of California, Davis, CA 95616

Edited by Carol Prives, Columbia University, New York, NY, and approved September 15, 2017 (received for review June 30, 2017)

WT p53 is critical for tumor suppression, whereas mutant p53 promotes tumor progression. Nerve injury-induced protein 1 (Ninj1) is a target of p53 and forms a feedback loop with p53 by repressing p53 mRNA translation. Here, we show that loss of *Ninj1* increased mutant p53 expression and, subsequently, enhanced cell growth and migration in cells carrying a mutant p53. In contrast, loss of *Ninj1* inhibited cell growth and migration in cells carrying a WT p53. To explore the biological significance of Ninj1, we generated a cohort of *Ninj1*-deficient mice and found that *Ninj1*^{+/-} mice were prone to systemic inflammation and insulinitis, but not to spontaneous tumors. We also found that loss of *Ninj1* altered the tumor susceptibility in both mutant p53 and p53-null background. Specifically, in a mutant p53(R270H) background, *Ninj1* deficiency shortened the lifespan, altered the tumor spectrum, and increased tumor burden, likely via enhanced expression of mutant p53. In a p53-null background, *Ninj1* deficiency significantly increased the incidence of T-lymphoblastic lymphoma. Taken together, our data suggest that depending on p53 genetic status, Ninj1 has two opposing functions in tumorigenesis and that the Ninj1–p53 loop may be targeted to manage inflammatory diseases and cancer.

Ninjurin 1 | mutant p53 | p53 | inflammation | cell adhesion

The tumor suppressor p53 is often referred to as the “guardian of the genome” and loss of p53 function is known to be central for tumor development (1, 2). The importance of p53 in tumor suppression is underscored by its ability as a transcription factor. In response to various stress signals, p53 is activated and then induces a plethora of target genes that mediate cell cycle arrest, apoptosis, and senescence (3). p53 is the most commonly mutated gene in human cancers (4). Unlike most tumor-suppressor genes that are mainly inactivated by deletion, the vast majority of tumor-derived p53 mutations are missense mutations and clustered within the central DNA-binding domain (5). Consequently, these mutations make p53 protein defective in DNA binding and loss of tumor suppression (6, 7). However, many p53 mutants acquire new and distinct oncogenic properties, generally referred to as gain-of-function, such as the ability to promote cell proliferation, metastasis, and chemoresistance (8, 9).

Cell adhesion molecules (CAMs) are typically transmembrane proteins and composed of an intracellular domain that mediates the intracellular signal pathways, a transmembrane domain, and an extracellular domain that interacts with the same CAMs (homophilic binding) or with different CAMs or extracellular matrix (heterophilic binding) (10). In addition to cell adhesion, CAMs serve as a biosensor to the changing surrounding microenvironment (10). As a result, CAMs are critical for many fundamental processes, such as cell and tissue homeostasis, tissue repair, and wound healing (11). In addition, altered function of CAMs have been implicated in tumor progression and metastasis (12).

Nerve injury-induced protein 1 (Ninjurin1, Ninj1) is a homophilic CAM and originally identified as a gene to be highly induced by nerve injury in Schwann cells and dorsal root ganglion (13).

Ninj1 is ubiquitously expressed in epithelial cells (14) and plays a role in the progression of multiple sclerosis (15) and migration of T cells to the intraluminal surface of blood vessels in the central nervous system of rodents with experimental autoimmune encephalomyelitis (EAE) (16). Conversely, *Ninj1* deficiency attenuates the severity of EAE in mice (17). Ninj1 also plays a role in angiogenesis by modulating neovessel formation in vitro (18) and the hyaloid vascular system in vivo (19). Additionally, inhibition of Ninj1 by a neutralizing Ninj1 antibody enhances penile angiogenesis and restores erectile function in streptozotocin-induced diabetic mice (20). Moreover, Ninj1 is capable of suppressing cancer cell invasion and migration in Ninj1-expressing cells and transgenic mice (21, 22). Previously, we showed that Ninj1 is a target of p53 and in turn regulates p53 mRNA translation (23). Here, we found that Ninj1 is capable of regulating mutant p53 expression. Most importantly, we found that Ninj1 exerts two opposing effects on cell growth, migration, and tumorigenesis via WT and mutant p53, respectively.

Results

The Effect of Ninj1 on Cell Growth and Migration Is Dependent on the Genetic Status of the p53 Gene. Previously, we showed that Ninj1 modulates WT p53 expression via mRNA translation (23). Thus, we explored whether mutant p53 is regulated by Ninj1 in SW480 and MIA-PaCa2 cells. SW480 cells contain one allele of the p53 gene with two mutations (R273H and P309S), whereas MIA-PaCa2 cells contain a mutant p53(R248W). The level of WT

Significance

Nerve injury-induced protein 1 (Ninj1), a p53 target, forms a feedback loop with p53 by repressing p53 translation. Here, we show that cell growth was enhanced by *Ninj1* deficiency in cells carrying a mutant p53, but inhibited in cells carrying a WT p53. We also show that in WT p53 background, *Ninj1*-deficient mice were prone to systemic inflammation, but not to spontaneous tumors. Importantly, loss of *Ninj1* altered lifespan and tumor susceptibility in mutant p53 and p53-null mice. Taken together, our results reveal a critical role of Ninj1 in p53-dependent tumor suppression and the Ninj1–p53 loop may be explored as a potential therapeutic target for the treatment of inflammatory diseases and cancers.

Author contributions: H.J.Y., J.Z., W.Y., S.-J.C., C.L., A.S., and W.Z. designed research; H.J.Y., J.Z., W.Y., S.-J.C., C.L., A.S., and W.Z. performed research; M.C. and E.C.H. designed histological research; M.C. and E.C.H. performed histological analysis; H.J.Y., J.Z., and X.C. analyzed data; and H.J.Y., J.Z., and X.C. wrote the paper.

The authors declare no conflict of interest.

This article is a PNAS Direct Submission.

Published under the PNAS license.

¹To whom correspondence may be addressed. Email: jinzhang@ucdavis.edu or xbchen@ucdavis.edu.

This article contains supporting information online at www.pnas.org/lookup/suppl/doi:10.1073/pnas.1711814114/-DCSupplemental.

p53 in MCF7 cells was measured as a control and found to be decreased upon ectopic expression of Ninj1 (Fig. 1A), consistent with our previous study (23). Similarly, upon ectopic expression of Ninj1, the level of mutant p53 was decreased in SW480 and MIA-PaCa2 cells (Fig. 1B and C). Moreover, Egr-1, a target of mutant p53 (24), was decreased by Ninj1 (Fig. 1B and C). Next, we examined the effect of endogenous Ninj1 on p53 expression in multiple cell lines in that the *NINJ1* gene was knocked out by CRISPR-Cas9 (SI Appendix, Fig. S1A). Sequencing analysis showed that Ninj1-KO MCF7 and MIA-PaCa2 cells had a 42-nt deletion in exon 1 of the *NINJ1* gene (SI Appendix, Fig. S1B and C). In contrast, Ninj1-KO SW480 cells had a 60-nt deletion in one allele and a 92-nt deletion in other allele (SI Appendix, Fig. S1B and C). Due to nonsense-mediated mRNA decay, Ninj1 protein was not detectable in these Ninj1-KO cells (Fig. 1D–F). In Ninj1-KO MCF7 cells, the level of p53 was increased (Fig. 1D). To verify that Ninj1 represses p53 translation, we showed that the binding of eIF4E to the p53 mRNA was increased by Ninj1 deficiency (SI Appendix, Fig. S2, compare lane 5 with 6), consistent with our previous observation (23). Moreover, we found that the levels of mutant p53 were increased by Ninj1-KO along with increased expression of Egr-1 in SW480 and MIA-PaCa2 cells (Fig. 1E and F).

WT p53 is a tumor suppressor, whereas mutant p53 acts as an oncogene (25). Thus, we speculated that the regulation of WT vs. mutant p53 by Ninj1 would result in two distinct biological responses. To test this, a colony formation assay was performed with isogenic controls and Ninj1-KO cells. We found that loss of Ninj1 reduced the number of colonies in MCF7 cells (Fig. 2A), consistent with our previous report (23). In contrast, loss of Ninj1 markedly increased the number of colonies in SW480 (Fig. 2B) and MIA-PaCa2 (Fig. 2C) cells. Next, a wound-healing assay was performed and showed that loss of Ninj1 inhibited cell migration in MCF7 cells (Fig. 2D). Conversely, cell migration was enhanced by loss of Ninj1 in both SW480 and MIA-PaCa2 cells (Fig. 2E and F). These results suggest that Ninj1 exerts two opposing functions in cell growth and migration via WT and mutant p53, respectively.

A 12-aa Ninj1-Blocking Peptide Elicits a Strong Effect on p53 Expression and Cell Growth. Pharmacological modulation of p53 expression is actively explored as a strategy for cancer therapy. Thus, we synthesized a 12-aa peptide corresponding to the N-terminal extracellular region of Ninj1 (SI Appendix, Fig. S3A), which is known to block homophilic interaction of Ninj1 (16). We found that upon treatment with the 12-aa peptide, the levels of WT and mutant p53 proteins were increased in isogenic controls, but not in Ninj1-KO MCF7 and MIA-PaCa2 cells (SI Appendix, Fig. S3B and D, compare lanes 1 and 3 with 2 and 4, respectively). We note that the basal levels of WT and mutant p53 were elevated by Ninj1-KO compared with that in isogenic controls (SI Appendix, Fig. S3B and D, compare lane 1 with 3). Additionally, we found that the number of colonies was decreased by the Ninj1-blocking peptide

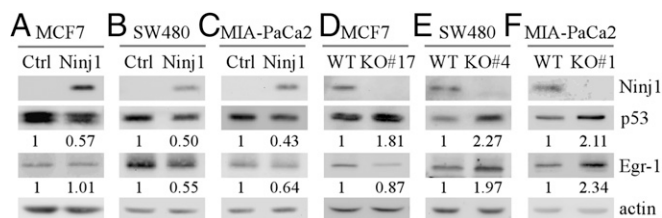


Fig. 1. Ninj1 regulates WT and mutant p53 expression. (A–C) Ninj1, p53, Egr-1, and actin proteins were examined by Western blotting in MCF7 (A), SW480 (B), and MIA-PaCa2 (C) cells transiently transfected with a control or Ninj1-expressing vector. (D–F) Ninj1, p53, Egr-1, and actin proteins were examined by Western blotting in isogenic controls and Ninj1-KO MCF7 (D), SW480 (E), and MIA-PaCa2 (F) cells.

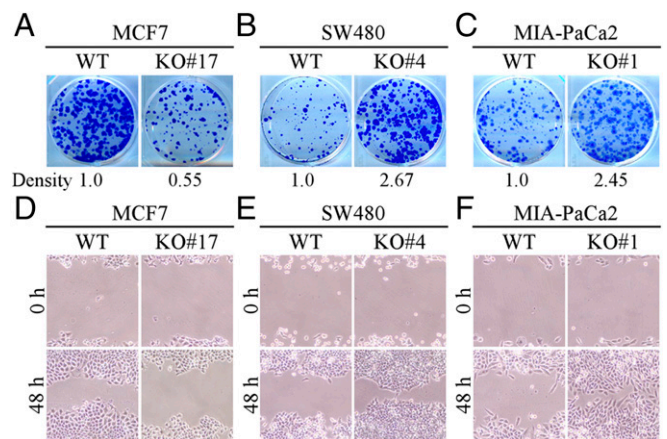


Fig. 2. The effect of Ninj1 on cell growth and migration is p53-dependent. (A–C) Colony formation assay was performed with isogenic controls, Ninj1-KO MCF7 (A), SW480 (B), and MIA-PaCa2 (C) cells. (D–F) Wound-healing assay was performed with isogenic controls and Ninj1-KO MCF7 (D), SW480 (E), and MIA-PaCa2 (F) cells. The images were proportionally scaled with an original magnification of 100 \times .

in MCF7 cells (SI Appendix, Fig. S3C), but increased in MIA-PaCa2 cells (SI Appendix, Fig. S3E). These data suggest that the effect of Ninj1-KO on p53 expression is recapitulated by the 12-aa Ninj1-blocking peptide.

Ninj1-Heterozygous Mice Are Prone to Systemic Inflammation. Previously, we showed that *Ninj1*-null mice succumb to hydrocephalus (23), and thus are not suitable for long-term study. In this regard, a cohort of WT ($n = 24$) and *Ninj1*^{+/-} ($n = 21$) mice was generated and monitored throughout their lifespan (SI Appendix, Tables S1 and S2). We note that 17 WT mice have been analyzed for another tumor study (26). We found that many *Ninj1*^{+/-} mice developed skin lesions (severe ulcerative psoriasiform dermatitis) and had to be killed. As a result, the median lifespan for *Ninj1*^{+/-} mice (98.71 wk) was shorter than—but still insignificant from—that for WT mice (120 wk; $P = 0.08$ by log-rank test) (Fig. 3A). If mice with skin lesions were excluded, the median survival for *Ninj1*^{+/-} mice ($n = 11$, 115 wk) was similar to that for WT mice ($n = 21$, 121 wk; $P = 0.695$ by log-rank test) (SI Appendix, Fig. S4A). In contrast, the incidence of ulcerative dermatitis was significantly higher in *Ninj1*^{+/-} mice than that in WT mice ($P = 0.0192$ by Fisher's exact test) (Fig. 3B). Next, histopathological analysis was performed and showed that some WT (5 of 24) and *Ninj1*^{+/-} (8 of 21) mice developed spontaneous tumors (SI Appendix, Tables S1 and S2). However, the tumor incidence between WT and *Ninj1*^{+/-} mice was not statistically significant ($P = 0.3234$ by Fisher's exact test).

Histopathological analysis indicates that the skin lesion in *Ninj1*^{+/-} mice exhibited marked psoriasiform epidermal hyperplasia and infiltrates of intradermal perivascular neutrophils and lymphohistiocytes along with multifocal ulceration (Fig. 3C). Moreover, we found that compared with WT mice, *Ninj1*^{+/-} mice were prone to systemic inflammation in the liver, kidney, salivary gland, pancreas, and lung (Fig. 3D, H&E staining panel, and SI Appendix, Fig. 4B and Tables S1 and S2). Immunohistochemistry (IHC) indicated that the chronic inflammatory infiltrates were composed of mixed CD3⁺ T and B220⁺ B cells along with a few macrophages (F4/80⁺) (Fig. 3D). Next, the levels of IL-6, a key cytokine known to stimulate inflammatory and autoimmune responses (27), were examined and found to be increased in the liver, kidney, and spleen of *Ninj1*^{+/-} mice compared with that in WT mice (Fig. 3E and F and SI Appendix, Fig. S4C). Similarly, the levels of several proinflammatory cytokines (TNF- α , IFN- γ , IL-8,

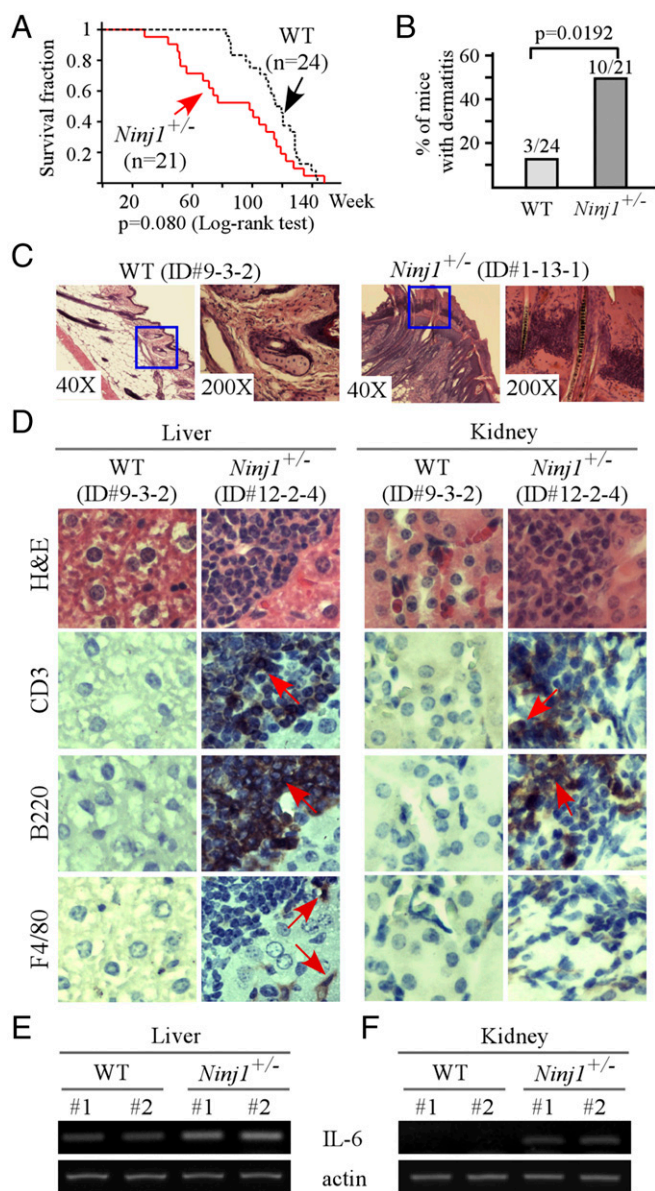


Fig. 3. Mice deficient in *Ninj1* are prone to systemic inflammation. (A) Kaplan-Meier survival curve for WT vs. *Ninj1*^{+/-} mice ($P = 0.080$ by log-rank test). (B) The percentage of mice with dermatitis in WT vs. *Ninj1*^{+/-} mice ($P = 0.0192$ by Fisher's exact test). (C) Representative images of H&E-stained skin sections from a pair of gender-matched WT and *Ninj1*^{+/-} mice. (D) Representative images of H&E- and IHC-stained liver and kidney sections from a pair of gender-matched WT and *Ninj1*^{+/-} mice. The red arrows indicate the positive-staining cells. The images were proportionally scaled with an original magnification of 200 \times . (E and F) IL-6 and actin transcripts were examined in the liver and kidney of two pairs of gender-matched WT and *Ninj1*^{+/-} mice. WT#1: F/56w/ID#5-19-3. WT#2: F/50w/ID#9-3-2. *Ninj1*^{+/-} #1: F/51w/ID#11-8-5. *Ninj1*^{+/-} #2: F/44w/ID#12-2-4.

and IL-1 β) were also increased by *Ninj1* deficiency (*SI Appendix*, Fig. S4D). These results suggest that *Ninj1* deficiency promotes infiltration of immune cells and enhances production of proinflammatory cytokines, resulting in systemic chronic inflammation.

Mice Deficient in *Ninj1* Are Prone to Pancreatic Insulinitis. When examining various organs of WT and *Ninj1*^{+/-} mice for inflammatory responses, we found that *Ninj1*^{+/-} mice had chronic pancreatic insulinitis with expanded lymphohistiocytic infiltrates surrounding the islets (Fig. 4A). The incidence of insulinitis was significantly

higher in *Ninj1*^{+/-} mice than in WT mice ($P = 0.0088$ by Fisher's exact test) (Fig. 4B and *SI Appendix*, Tables S1 and S2). We would like to mention that insulinitis is a hallmark of type I diabetes, a T cell-mediated autoimmune disease characterized by selective destruction of pancreatic insulin-secreting β -cells (28). Because T cells are not a constitutive component of normal islets, the infiltration of T cells to islets represents a prerequisite for development of autoimmune type I diabetes (28). Thus, IHC analysis was performed to confirm that normal islets from a WT mouse were essentially negative for inflammatory cells (Fig. 4C). However, a mixed T and B cell population was detected surrounding the islets from a *Ninj1*^{+/-} mouse with histological features typical of insulinitis (Fig. 4D). Interestingly, the immune cells within the islets were predominantly T cells (Fig. 4D).

***Ninj1* Deficiency Shortens the Lifespan, Increases the Tumor Burden, and Alters the Tumor Spectrum in *p53*^{R270H/-} Mice.** To examine whether *Ninj1* has an effect on mutant *p53*-mediated tumorigenesis, we generated a cohort of *p53*^{R270H/-} ($n = 31$) and *Ninj1*^{+/-}; *p53*^{R270H/-} ($n = 28$) mice (*SI Appendix*, Tables S3 and S4). Murine *p53*(R270H) corresponds to human *p53*(R273H), a gain-of-function mutant (7, 29). All mice succumbed to tumors, except for two *p53*^{R270H/-} mice who died because of an unknown reason (*SI Appendix*, Tables S3 and S4). We found that the median survival for *p53*^{R270H/-} mice was 26.71 wk, which was shortened to 23.14 wk in *Ninj1*^{+/-}; *p53*^{R270H/-} mice ($P = 0.014$ by log-rank test) (Fig. 5A). In addition, histopathological analysis indicated that

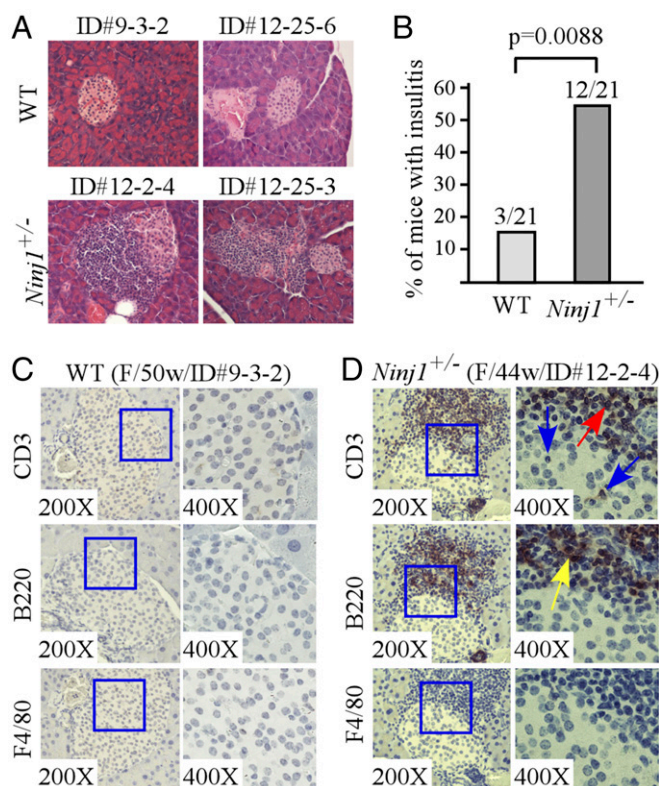


Fig. 4. Mice deficient in *Ninj1* are prone to insulinitis. (A) Representative images of H&E-stained pancreas sections from two pairs of gender-matched WT and *Ninj1*^{+/-} mice. The images were proportionally scaled with an original magnification of 200 \times . (B) The incidence of insulinitis in WT vs. *Ninj1*^{+/-} mice ($P = 0.0088$ by Fisher's exact test). (C and D) Pancreas sections from WT (C) and *Ninj1*^{+/-} (D) mice were stained with antibodies against CD3, B220, or F4/80. The box plots were used to show the staining area in the right. Red arrow: T cells at the inflammation site. Blue arrow: T cells inside the islet. Yellow arrow: B cells at the inflammation site.

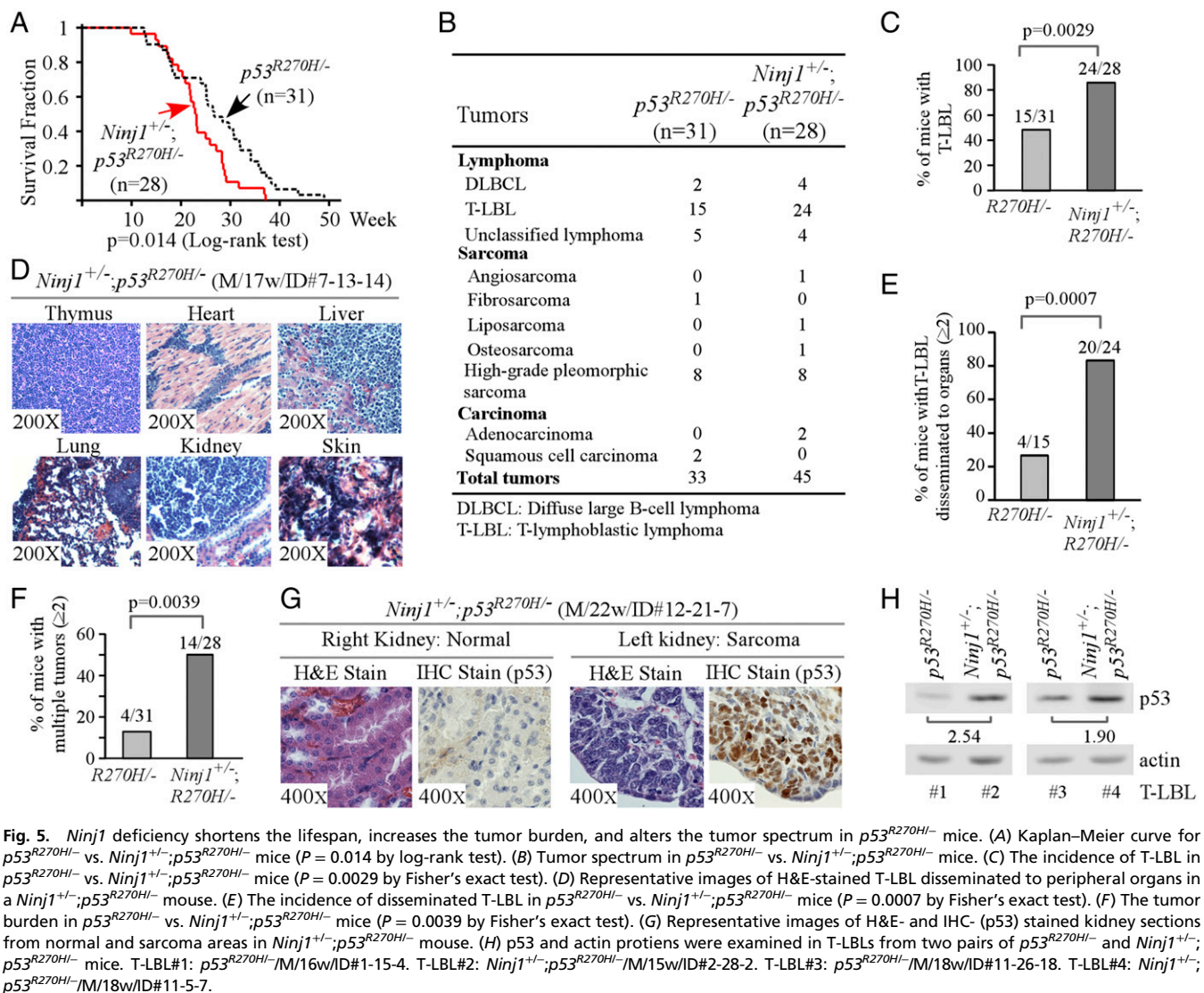


Fig. 5. *Ninj1* deficiency shortens the lifespan, increases the tumor burden, and alters the tumor spectrum in $p53^{R270H/-}$ mice. (A) Kaplan–Meier curve for $p53^{R270H/-}$ vs. $Ninj1^{+/-}; p53^{R270H/-}$ mice ($P = 0.014$ by log-rank test). (B) Tumor spectrum in $p53^{R270H/-}$ vs. $Ninj1^{+/-}; p53^{R270H/-}$ mice. (C) The incidence of T-LBL in $p53^{R270H/-}$ vs. $Ninj1^{+/-}; p53^{R270H/-}$ mice ($P = 0.0029$ by Fisher’s exact test). (D) Representative images of H&E-stained T-LBL disseminated to peripheral organs in a $Ninj1^{+/-}; p53^{R270H/-}$ mouse. (E) The incidence of disseminated T-LBL in $p53^{R270H/-}$ vs. $Ninj1^{+/-}; p53^{R270H/-}$ mice ($P = 0.0007$ by Fisher’s exact test). (F) The tumor burden in $p53^{R270H/-}$ vs. $Ninj1^{+/-}; p53^{R270H/-}$ mice ($P = 0.0039$ by Fisher’s exact test). (G) Representative images of H&E- and IHC- (p53) stained kidney sections from normal and sarcoma areas in $Ninj1^{+/-}; p53^{R270H/-}$ mouse. (H) p53 and actin proteins were examined in T-LBLs from two pairs of $p53^{R270H/-}$ and $Ninj1^{+/-}; p53^{R270H/-}$ mice. T-LBL#1: $p53^{R270H/-}$ /M/16w/ID#1-15-4. T-LBL#2: $Ninj1^{+/-}; p53^{R270H/-}$ /M/15w/ID#2-28-2. T-LBL#3: $p53^{R270H/-}$ /M/18w/ID#11-26-18. T-LBL#4: $Ninj1^{+/-}; p53^{R270H/-}$ /M/18w/ID#11-5-7.

Ninj1 heterozygosity altered the tumor spectrum in $p53^{R270H/-}$ mice (Fig. 5B and *SI Appendix*, Tables S3 and S4). The penetrance of T-lymphoblastic lymphoma (T-LBL) was significantly higher in $Ninj1^{+/-}; p53^{R270H/-}$ mice (24 of 28) than that in the $p53^{R270H/-}$ mice (15 of 31; $P = 0.0029$ by Fisher’s exact test) (Fig. 5C). Additionally, we found that T-LBLs developed in $Ninj1^{+/-}; p53^{R270H/-}$ mice were disseminated to multiple organs, including the heart, kidney, skin, liver, and lung (20 of 24 for $Ninj1^{+/-}; p53^{R270H/-}$ mice vs. 4 of 15 for $p53^{R270H/-}$ mice; $P = 0.0007$ by Fisher’s exact test) (Fig. 5D and E). Moreover, the number of mice with two or more tumors derived from two different cell lineages was significantly higher in $Ninj1^{+/-}; p53^{R270H/-}$ (14 of 28) mice than that in $p53^{R270H/-}$ (4 of 31) mice ($P = 0.0039$ by Fisher’s exact test) (Fig. 5F and *SI Appendix*, Fig. S5A and Tables S3 and S4). We would like to note that several types of tumors, such as angiosarcoma, liposarcoma, osteosarcoma, and adenocarcinoma, were only detected in $Ninj1^{+/-}; p53^{R270H/-}$ but not in $p53^{R270H/-}$ mice (Fig. 5B and *SI Appendix*, Fig. S5B and Tables S3 and S4). Similarly, fibrosarcoma and squamous cell carcinoma developed in $p53^{R270H/-}$ mice were not found in $Ninj1^{+/-}; p53^{R270H/-}$ mice (Fig. 5B and *SI Appendix*, Tables S3 and S4).

Next, IHC analysis was performed to examine mutant p53 expression in normal and tumor tissues from $Ninj1^{+/-}; p53^{R270H/-}$ mice. We found that mutant p53 protein was detected in the tumor tissues but not in the normal tissues from $Ninj1^{+/-}; p53^{R270H/-}$

mice (Fig. 5G and *SI Appendix*, Fig. S6). In addition, in the tumor tissues, only tumor cells, but not intratumoral stromal cells, were positive in p53 staining (Fig. 5G and *SI Appendix*, Fig. S6). These observations are consistent with a previous report that mutant p53 protein was highly expressed in tumor cells from $p53^{R172H}$ -knockin mice (30). Moreover, to determine whether the aggressive tumor phenotypes observed in $Ninj1^{+/-}; p53^{R270H/-}$ mice are due to increased expression of mutant p53 by *Ninj1* deficiency, we measured the levels of mutant p53 protein in the T-LBLs derived from two pairs of gender-matched $p53^{R270H/-}$ and $Ninj1^{+/-}; p53^{R270H/-}$ mice. Indeed, we found that the levels of mutant p53 were much higher in the T-LBLs from $Ninj1^{+/-}; p53^{R270H/-}$ mice than that from $p53^{R270H/-}$ mice (Fig. 5H). To verify this, mouse embryo fibroblasts (MEFs) were isolated and showed that the level of mutant p53(R270H) protein was much higher in $Ninj1^{-/-}; p53^{R270H/-}$ MEFs than that in $p53^{R270H/-}$ MEFs (*SI Appendix*, Fig. S5C). These results were consistent with the above observations that *Ninj1* deficiency increased mutant p53 expression in SW480 and MIA-PaCa2 cells (Fig. 1E and F). Since mutant p53 is known to create a permissive tumor microenvironment via enhancing protumor inflammation (31), we examined the levels of proinflammatory cytokines, including TNF- α , IFN- γ , IL-8, IL-6, and IL-1 β , in the T-LBLs from $p53^{R270H/-}$ and $Ninj1^{+/-}; p53^{R270H/-}$ mice. We found that the

levels of these proinflammatory cytokines were all increased in *Ninj1*^{+/-};*p53*^{R270H/-} T-LBLs compared with that in *p53*^{R270H/-} T-LBLs (*SI Appendix*, Fig. S7).

Ninj1 Deficiency Increases the Penetrance of T-LBL in *p53*-Null Mice.

While *Ninj1*^{+/-} mice were susceptible to systemic inflammation, these mice were still not prone to spontaneous tumors (*SI Appendix*, Table S2), suggesting that increased expression of WT p53 by *Ninj1* deficiency may have tempered inflammation-induced tumorigenesis. Thus, we sought to determine whether *Ninj1* deficiency plays a role in tumorigenesis independent of p53. To test this, we generated a cohort of *p53*^{-/-} and *Ninj1*^{+/-};*p53*^{-/-} mice. We would like to mention that except for one animal, 24 *p53*^{-/-} mice used as control were analyzed in a previous study (26). All mice succumbed to tumors, with the exception of two *Ninj1*^{+/-};*p53*^{-/-} mice that died from hydrocephalus (*SI Appendix*, Tables S5 and S6). The median survival for *Ninj1*^{+/-};*p53*^{-/-} mice (19.43 wk) was shorter than—but still insignificant from—that for *p53*^{-/-} mice (24 wk; $P = 0.669$ by log-rank test) (Fig. 6A). Histopathological analysis showed that *Ninj1*^{+/-};*p53*^{-/-} mice were prone to T-LBL (Fig. 6B and C and *SI Appendix*, Table S6). Statistical analysis indicated that the penetrance of T-LBL was significantly higher in *Ninj1*^{+/-};*p53*^{-/-} mice (21 of 24) compared with *p53*^{-/-} mice (12 of 25; $P = 0.0054$ by Fisher's exact test) (Fig. 6B). Additionally, *Ninj1*^{+/-};*p53*^{-/-} mice did not develop hibernoma, hemangioma, granulocytic sarcoma, histiocytic sarcoma, osteosarcoma, and rhabdomyosarcoma (Fig. 6C and *SI Appendix*, Table S6). Instead, *Ninj1*^{+/-};*p53*^{-/-} mice

developed high-grade pleomorphic sarcoma, which was not observed in *p53*^{-/-} mice (Fig. 6C and *SI Appendix*, Tables S5 and S6).

Discussion

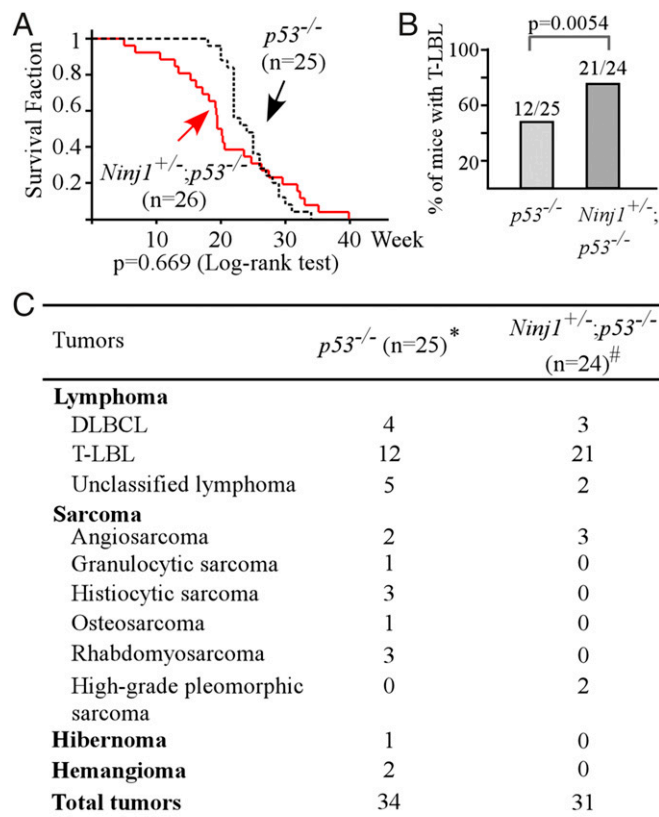
Ninj1 is a target of p53 and found to repress WT p53 expression via mRNA translation (23). In the present study, we extended our work to investigate the role of the *Ninj1*-p53 loop in vivo. We showed that *Ninj1* is capable of modulating mutant p53 expression (Fig. 1). Interestingly, depending on the genetic status of the *p53* gene, cell proliferation and migration can be inhibited by the loss of *Ninj1* in cells carrying a WT p53, but increased in cells carrying a mutant p53 (Fig. 2). We also showed that in the WT *p53* background, mice deficient in *Ninj1* are not prone to spontaneous tumors (*SI Appendix*, Tables S1 and S2). However, in a mutant *p53*^{R270H/-} background, mice deficient in *Ninj1* have a shorter lifespan and are prone to aggressive tumors (Fig. 5 and *SI Appendix*, Tables S3 and S4). Because *Ninj1* deficiency leads to increased expression of WT and mutant p53, we conclude that *Ninj1* has two opposing functions in tumorigenesis via WT and mutant p53, respectively.

Here, we found that *Ninj1*-deficient mice are prone to systemic chronic inflammation in the skin, liver, kidney, and pancreas (Figs. 3 and 4 and *SI Appendix*, Fig. S4 B–D and Tables S1 and S2). We also showed that the immune cells at the inflammation sites were mainly T and B cells (Figs. 3D and 4D). In addition, we showed that the levels of proinflammatory cytokines were increased in the *Ninj1*^{+/-} mice tissues compared with that in the WT mice tissues (Fig. 3E and F and *SI Appendix*, Fig. S4 C and D). We speculate that loss of *Ninj1* would attenuate the cell-adhesion activities and, subsequently, promote migration of T and B cells. Thus, additional studies are warranted to address the role of *Ninj1* in modulating the immune responses.

Recent advances have highlighted a role for WT p53 in the inflammatory response as a part of its tumor-suppressor activity (32). In contrast, mutant p53 fuels protumor inflammation and promotes inflammation-induced tumor progression through enhanced secretion of chemokines by tumor cells carrying mutant p53 (31). We showed that *Ninj1*-het mice with an intact *p53* remain near normal in terms of tumor formation. However, in a mutant *p53* or *p53*-null background, *Ninj1* deficiency creates a permissive microenvironment and synergizes with loss of *p53* or mutant *p53* to promote tumor progression and metastasis. In support of this notion, we showed that the incidence of T-LBL is markedly increased by *Ninj1* deficiency in *Ninj1*^{+/-};*p53*^{R270H/-} and *Ninj1*^{+/-};*p53*^{-/-} mice (Figs. 5C and 6B, and *SI Appendix*, Tables S3–S6). Consistent with this, the levels of proinflammatory cytokines (TNF- α , IFN- γ , IL-8, IL-6, and IL-1 β) were increased by *Ninj1* deficiency in *Ninj1*^{+/-};*p53*^{R270H/-} T-LBLs (*SI Appendix*, Fig. S7).

Insulinitis is an inflammatory response surrounding or within pancreatic islets and often found in patients with autoimmune type I and II diabetes (33). Here, we found that mice deficient in *Ninj1* are prone to insulinitis along with predominantly T cell infiltration within the islet and mixed accumulation of T and B cells surrounding the islet (Fig. 4). Because *Ninj1*^{+/-} mice are prone to systemic inflammation, it is likely that the systemic inflammation serves as a contributing factor to the increased incidence of insulinitis. However, it remains unclear whether the insulinitis-prone *Ninj1*-deficient mice will develop type I diabetes. Additionally, as p53 plays a role in pancreatic β -cell apoptosis via p53 up-regulated modulator of apoptosis (34), future studies are warranted to determine whether increased expression of p53 by *Ninj1* deficiency is involved in the insulinitis and pancreatic β -cell death.

We showed that a 12-aa *Ninj1*-blocking peptide has an opposing effect on cell proliferation: through up-regulation of WT p53 to inhibit cell growth in MCF7 cells (*SI Appendix*, Fig. S3 B and C) and through up-regulation of mutant p53 to promote cell



* 24 of *p53*-KO mice were from a published study (PNAS 111:18637-42).

[#]Two mice with hydrocephalus were excluded.

Fig. 6. *Ninj1* deficiency increases the penetrance of T-LBL in *p53*^{-/-} mice. (A) Kaplan-Meier curve for *p53*^{-/-} vs. *Ninj1*^{+/-};*p53*^{-/-} mice ($P = 0.669$ by log-rank test). (B) The incidence of T-LBL in *p53*^{-/-} vs. *Ninj1*^{+/-};*p53*^{-/-} mice ($P = 0.0054$ by Fisher's exact test). (C) Tumor spectrum in *p53*^{-/-} vs. *Ninj1*^{+/-};*p53*^{-/-} mice.

growth in MIA-PaCa2 cells (*SI Appendix, Fig. S3 D and E*). Consistent with this finding, a previous report showed that the Ninj1-blocking peptide inhibits T cell migration in the vessels in a rat EAE model (16). However, the Ninj1-blocking peptide is also found to alleviate inflammatory response in a septic model (35), which seems to contradict the observations in this study and by an earlier report (16). One possible explanation is simply due to the mouse models used: *Ninj1*-deficient mouse model for this study and rat EAE model for one early report (16) vs. a septic mouse model for the other study (35). The other possibility is that *Ninj1* deficiency in our mouse model may have a long-term and systemic effect on the immune systems, whereas the Ninj1-blocking peptide may exert a transient effect on the immune systems in septic mice. Thus, additional studies are needed to determine the role of the Ninj1-blocking peptide in inflammatory responses and in p53-dependent tumor suppression *in vitro* and *in vivo*.

Materials and Methods

Cell Lines and Primary Mouse MEFs. MCF7, SW480, and MIA-PaCa2 cells were cultured in DMEM (Invitrogen) supplemented with 10% FBS (HyClone). To generate *Ninj1*-KO cell lines using the CRISPR/Cas9 system, we followed the previously described protocol (36). Individual single-guide RNA constructs targeting *Ninj1* (*SI Appendix, Fig. S1A*) were cloned into the pSpCas9(BB)-2A-Puro (PX459) vector (Addgene). Upon transfection of the targeting vector into cells, *Ninj1*-KO clones were selected by puromycin and confirmed by sequencing. *p53^{R270H/-}* and *Ninj1^{+/-};p53^{R270H/-}* MEFs were isolated from 13.5-d embryos as described previously (37).

Mice Deficient in *Ninj1*, *p53*, or Carrying a *p53^{R270H}* Knockin Allele. *Ninj1*-deficient mice were generated as described previously (23). *p53^{+/-}* and *p53^{R270H/+}* knockin mice (38) were purchased from the Jackson Laboratory. *Ninj1^{+/-};p53^{+/-}* mice were crossed with *p53^{+/-}* or *p53^{R270H/+}* mice to generate *Ninj1^{+/-};p53^{+/-}* or *Ninj1^{+/-};p53^{R270H/-}* mice. All animals and experimental protocols were

approved by the University of California, Davis Institutional Animal Care and Use Committee. To genotype *Ninj1* and *p53*-deficient mice, the primers were used as previously described (23, 39). To test *p53^{R270H}* knockin allele, the primers are 5'-AGC CTG CCT AGC TTC CTC AGG-3' and 5'-CTT GGA GAC ATA GCC ACA CTG-3'.

Histological Analysis. Tissue processing, H&E staining, and IHC analysis were performed as previously described (26).

RNA Isolation and RT-PCR Analysis. Total RNAs were purified with TRIzol (Invitrogen) and then subjected to cDNA synthesis using M-MLV reverse transcriptase (Promega). The program used for amplification was: (i) 94 °C for 5 min, (ii) 94 °C for 45 s, (iii) 58 °C for 45 s, (iv) 72 °C for 1 min, and (v) 72 °C for 10 min. The primers to detect *murine IL-6* are 5'-GAG GAT ACC ACT CCC AAC AGA CC-3' and 5'-AAG TGC ATC ATC GTT GTT CAT ACA-3'; and for *murine actin*, 5'-CCC ATC TAC GAG GGC TAT-3' and 5'-AGA AGG AAG GCT GGA AAA-3'.

Western Blot Analysis and Colony Formation Assay. Western blotting was performed as described previously (23) with anti-human p53 (DO-1; monoclonal), anti-p53 (Santa Cruz), anti-Egr-1 (Santa Cruz), anti-Ninj1 (Abcam), and antiactin (Sigma). Colony formation assay was also carried out as described previously (23).

Wound-Healing Assay. Cells were scratched with a 200- μ L pipette tip at 70% confluency, incubated with fresh medium for 48 h and then captured with Nikon microscope (Nikon Corporation).

Statistical Analysis. Fisher's exact test was used for comparison between two genotypes. Log-rank test was used to determine the difference in median survival between two genotypes.

ACKNOWLEDGMENTS. This work is supported in part by American Cancer Society Institutional Research Grant IRG-95-125-13 (to J.Z.) and by NIH Grant CA076069 (to X.C.).

- Vogelstein B, Lane D, Levine AJ (2000) Surfing the p53 network. *Nature* 408:307–310.
- Vousden KH, Prives C (2009) Blinded by the light: The growing complexity of p53. *Cell* 137:413–431.
- Harms K, Nozell S, Chen X (2004) The common and distinct target genes of the p53 family transcription factors. *Cell Mol Life Sci* 61:822–842.
- Kandoth C, et al. (2013) Mutational landscape and significance across 12 major cancer types. *Nature* 502:333–339.
- Olivier M, et al. (2002) The IARC TP53 database: New online mutation analysis and recommendations to users. *Hum Mutat* 19:607–614.
- Brosh R, Rotter V (2009) When mutants gain new powers: News from the mutant p53 field. *Nat Rev Cancer* 9:701–713.
- Ko LJ, Prives C (1996) p53: Puzzle and paradigm. *Genes Dev* 10:1054–1072.
- Oren M, Rotter V (2010) Mutant p53 gain-of-function in cancer. *Cold Spring Harb Perspect Biol* 2:a001107.
- Muller PA, Vousden KH (2014) Mutant p53 in cancer: New functions and therapeutic opportunities. *Cancer Cell* 25:304–317.
- Cavallaro U, Dejana E (2011) Adhesion molecule signalling: Not always a sticky business. *Nat Rev Mol Cell Biol* 12:189–197.
- Jacinto A, Martinez-Arias A, Martin P (2001) Mechanisms of epithelial fusion and repair. *Nat Cell Biol* 3:E117–E123.
- Makrilia N, Kollias A, Manolopoulos L, Syrigos K (2009) Cell adhesion molecules: Role and clinical significance in cancer. *Cancer Invest* 27:1023–1037.
- Araki T, Milbrandt J (1996) Ninjurin, a novel adhesion molecule, is induced by nerve injury and promotes axonal growth. *Neuron* 17:353–361.
- Araki T, Zimonjic DB, Popescu NC, Milbrandt J (1997) Mechanism of homophilic binding mediated by ninjurin, a novel widely expressed adhesion molecule. *J Biol Chem* 272:21373–21380.
- Ifergan I, et al. (2011) Role of Ninjurin-1 in the migration of myeloid cells to central nervous system inflammatory lesions. *Ann Neurol* 70:751–763.
- Odoardi F, et al. (2012) T cells become licensed in the lung to enter the central nervous system. *Nature* 488:675–679.
- Ahn BJ, et al. (2014) Ninjurin1 deficiency attenuates susceptibility of experimental autoimmune encephalomyelitis in mice. *J Biol Chem* 289:3328–3338.
- Matsuki M, et al. (2015) Ninjurin1 is a novel factor to regulate angiogenesis through the function of pericytes. *Circ J* 79:1363–1371.
- Lee HJ, et al. (2009) Ninjurin1 mediates macrophage-induced programmed cell death during early ocular development. *Cell Death Differ* 16:1395–1407.
- Yin GN, et al. (2014) Inhibition of Ninjurin 1 restores erectile function through dual angiogenic and neurotrophic effects in the diabetic mouse. *Proc Natl Acad Sci USA* 111:E2731–E2740.
- Woo JK, et al. (2016) Ninjurin1 inhibits colitis-mediated colon cancer development and growth by suppression of macrophage infiltration through repression of FAK signaling. *Oncotarget* 7:29592–29604.
- Jang YS, et al. (2016) Ninjurin1 suppresses metastatic property of lung cancer cells through inhibition of interleukin 6 signaling pathway. *Int J Cancer* 139:383–395.
- Cho SJ, et al. (2013) Ninjurin1, a target of p53, regulates p53 expression and p53-dependent cell survival, senescence, and radiation-induced mortality. *Proc Natl Acad Sci USA* 110:9362–9367.
- Weisz L, et al. (2004) Transactivation of the EGR1 gene contributes to mutant p53 gain of function. *Cancer Res* 64:8318–8327.
- Freed-Pastor WA, Prives C (2012) Mutant p53: One name, many proteins. *Genes Dev* 26:1268–1286.
- Zhang J, et al. (2014) Mice deficient in Rbm38, a target of the p53 family, are susceptible to accelerated aging and spontaneous tumors. *Proc Natl Acad Sci USA* 111:18637–18642.
- Neurath MF, Finotto S (2011) IL-6 signaling in autoimmunity, chronic inflammation and inflammation-associated cancer. *Cytokine Growth Factor Rev* 22:83–89.
- Frigerio S, et al. (2002) Beta cells are responsible for CXCR3-mediated T-cell infiltration in insulinitis. *Nat Med* 8:1414–1420.
- Yan W, Liu G, Scoumanne A, Chen X (2008) Suppression of inhibitor of differentiation 2, a target of mutant p53, is required for gain-of-function mutations. *Cancer Res* 68:6789–6796.
- Terzian T, et al. (2008) The inherent instability of mutant p53 is alleviated by Mdm2 or p16INK4a loss. *Genes Dev* 22:1337–1344.
- Di Minin G, et al. (2014) Mutant p53 reprograms TNF signaling in cancer cells through interaction with the tumor suppressor DAB2IP. *Mol Cell* 56:617–629.
- Takaoka A, et al. (2003) Integration of interferon-alpha/beta signalling to p53 responses in tumour suppression and antiviral defence. *Nature* 424:516–523.
- In't Veld P (2011) Insulinitis in human type 1 diabetes: The quest for an elusive lesion. *Islets* 3:131–138.
- Grzov EN, et al. (2010) p53 up-regulated modulator of apoptosis (PUMA) activation contributes to pancreatic beta-cell apoptosis induced by proinflammatory cytokines and endoplasmic reticulum stress. *J Biol Chem* 285:19910–19920.
- Jennewein C, et al. (2015) Contribution of Ninjurin1 to toll-like receptor 4 signaling and systemic inflammation. *Am J Respir Cell Mol Biol* 53:656–663.
- Ran FA, et al. (2013) Genome engineering using the CRISPR-Cas9 system. *Nat Protoc* 8:2281–2308.
- Scoumanne A, Cho SJ, Zhang J, Chen X (2011) The cyclin-dependent kinase inhibitor p21 is regulated by RNA-binding protein PCBP4 via mRNA stability. *Nucleic Acids Res* 39:213–224.
- Olive KP, et al. (2004) Mutant p53 gain of function in two mouse models of Li-Fraumeni syndrome. *Cell* 119:847–860.
- Zhang J, et al. (2011) Translational repression of p53 by RNPC1, a p53 target over-expressed in lymphomas. *Genes Dev* 25:1528–1543.